

**PREPRINT**

*Author-formatted, not peer-reviewed document posted on 04/05/2026*

DOI: <https://doi.org/10.3897/arphapreprints.e197963>

---

# **High-resolution tomographic analysis reveals complex dental microanatomy in *Psittacosaurus***

Yin Yalei, Buyu Wu, Zixian Sui, Junwei Xing,  Qi Zhao, Shuai Shao,  Xing Xu

1 **High-resolution tomographic analysis reveals complex dental microanatomy in**  
2 ***Psittacosaurus***

3

4 Ya-Lei Yin<sup>1,2,3,4,5</sup>, Bu-Yu Wu<sup>2</sup>, Zi-Xian Sui<sup>2</sup>, Jun-Wei Xing<sup>2</sup>, Qi Zhao<sup>6\*</sup>, Shuai Shao<sup>2</sup>,  
5 Xing Xu<sup>1,6\*</sup>

6

7 1 *Center for Vertebrate Evolutionary Biology, School of Life Sciences, Yunnan*  
8 *University, Kunming 650500, China*

9 2 *College of Paleontology, Shenyang Normal University, Shenyang 110034, China*

10 3 *Key Laboratory of Evolution of Past Life in NE Asia, Ministry of Natural Resources,*  
11 *Shenyang 110034, China*

12 4 *Key Laboratory of Evolutionary Systematics of Vertebrates, Institute of Vertebrate*  
13 *Paleontology and Paleoanthropology, Chinese Academy of Sciences, Beijing 100044,*  
14 *China*

15 5 *Observation and Research Station of Stratigraphy, Paleontology and Environmental*  
16 *Geology in Chaohu, MNR, No.999 Xianlonghu Road, Hefei 230001, China*

17 6 *Key Laboratory of Evolutionary Systematics of Vertebrates, Institute of Vertebrate*  
18 *Paleontology and Paleoanthropology, Chinese Academy of Sciences, Beijing 100044,*  
19 *China*

20

21 \*Corresponding authors: Xing Xu (xu.xing@ivpp.ac.cn); Qi Zhao  
22 (zhaoqi@ivpp.ac.cn).

23

24 **Abstract**

25

26 *Psittacosaurus* is known as the genus with the greatest number of species, among  
27 non-avian dinosaurs, with hundreds to thousands of specimens discovered throughout  
28 Asia. Nevertheless, the anatomical characteristics of *Psittacosaurus* teeth have not  
29 been thoroughly examined in previous research, limiting our understanding of its  
30 taxonomy. This study employs high-resolution computed tomography data to  
31 reconstruct and analyse the morphology of a left dentary tooth of *Psittacosaurus*  
32 discovered from the Lower Cretaceous Jiufotang Formation in Longcheng, Chaoyang,  
33 western Liaoning, China, which represents a new fossil site for psittacosaurus within  
34 the Jehol Biota. The reconstruction has revealed varied features of *Psittacosaurus*  
35 dentary teeth. These features include a distally angled bulbous primary ridge,  
36 secondary ridges present on the primary ridge of the crown, a median labial  
37 depression extending to the base of the crown, and a cingulum restricted on the distal  
38 lobe. Importantly, the reconstruction provides the first high-fidelity, three-dimensional  
39 visualization of a ceratopsian pulp cavity, which is characterized by a chisel-shaped  
40 pulp chamber and a columnar pulp canal. Our findings highlight the potential of  
41 non-destructive, high-resolution tomographic methods to uncover hidden anatomical  
42 complexity in well-studied fossil groups.

43

44 **Keywords**

45

46 Dentine, Jehol Biota, Jiufotang Formation, *Psittacosaurus*, tooth

47

48 **Introduction**

49

50 *Psittacosaurus* (psittacosaur) represents an early-diverging ceratopsian and is one  
51 of the most extensively sampled non-avian dinosaur genera, with numerous  
52 well-preserved specimens documented across the Early Cretaceous deposits of Asia  
53 (Serenó 1990, 2010; You and Dodson 2004; Zhao et al. 2013). Its dentition has been  
54 widely studied in terms of external morphology, including features such as  
55 asymmetrical enamel distribution, a bulbous primary ridge on dentary crowns, and  
56 broad wear surfaces (e.g. You and Dodson 2004; Sereno 2010). However, despite the  
57 abundance of material, and the potential taxonomic and phylogenetic significance of  
58 dental characters, the internal structure and developmental organization of  
59 psittacosaur teeth remain poorly understood.

60

61 The Jehol Biota of northeastern China has yielded numerous exceptionally  
62 well-preserved psittacosaurid fossils from the Yixian Formation located in Beipiao  
63 City (e.g., Xu and Wang 1998; Mayr et al. 2002; Zhao et al. 2014; Bullar et al. 2019;  
64 Zhao et al. 2019) and Chifeng City (Zhang et al. 2022), and the Jiufotang Formation  
65 in Chaoyang County (Serenó et al. 1988). Here, we report a new psittacosaur tooth  
66 from the Lower Cretaceous Jiufotang Formation in Longcheng District, Chaoyang  
67 City, western Liaoning Province, China, representing a new fossil site of  
68 psittacosaurids within this well-known biota, where two distinct types of saurischian  
69 teeth have previously been documented (Yin et al. 2025). Using high-resolution  
70 computed tomography (2.56  $\mu\text{m}$  voxel size), this research overcomes previous  
71 observational limits to deliver an unprecedented anatomical description of both the  
72 external and internal features of the tooth, and to discuss their taxonomic implications.

73

74 **Material and methods**

75

76 PMOL-ADt0008 is an isolated left dentary tooth specimen. The specimen  
77 examined in this study was obtained from the Jiufotang Formation of the Lower  
78 Cretaceous at Shangshuiquan Village, Lianhe Town, Longcheng District, Chaoyang  
79 City, western Liaoning Province, China (Fig. 1). This collection occurred during our  
80 field expedition on April, 2024. It is presently housed in the Paleontological Museum  
81 of Liaoning (PMOL).

82

83 The specimen PMOL-ADt0008 was prepared utilizing a steel needle under a Leica  
84 S6 microscope. Following this, imaging of the specimen was conducted with an  
85 Olympus DSX1000 located at the Paleontological Museum of Liaoning. The  
86 specimen PMOL-ADt0008 underwent CT scanning at Yinghua NDT (Shanghai) Co.,  
87 Ltd., using the Phoenix V|tome|x M240. This process generated 2201 projections at a  
88 voltage of 100 kV and a current of 200  $\mu\text{A}$ , with a voxel size of  $2.56 \times 2.56 \times 2.56 \mu\text{m}$ .

89 Segmentation and three-dimensional reconstruction of the data were executed using  
 90 VG STUDIO MAX 3.4 software (Volume Graphics, Heidelberg, Germany).

91

92 **Systematic Palaeontology**

93

94 **Dinosauria Owen, 1842**

95 **Ornithischia Seeley, 1887**

96 **Ceratopsia Marsh, 1890**

97 **Psittacosauridae Osborn, 1923**

98

99 ***Psittacosaurus* Osborn, 1923**

100

101 ***Psittacosaurus* sp.**

102

103 Material—PMOL-ADt0008, one isolated left dentary tooth (Figs 2–5).

104 Horizon—Lower Cretaceous Jiufotang Formation.

105

106 **Description**

107

108 PMOL-ADt0008 is a left dentary tooth, characterized by a bulbous primary ridge  
 109 angling distally and the presence of wear facets on the labial surface of the crown. It  
 110 comprises an almost complete tooth crown along with the basal portion of the root (Figs  
 111 2–3). This specimen is identified as a functional tooth, as indicated by the wear surfaces  
 112 observed on its crown. The tooth measures 6.5 mm in preserved length. The crown  
 113 exhibits a greater mesiodistal length compared to the root (Fig. 2), and its base is  
 114 slightly labial expanded relative to the root (Fig. 3A–D).

115

116 **Crown.** The crown exhibits a greater length than width, as in other early-diverging  
 117 ceratopsians (Tanoue et al. 2009). It measures approximately 5.8 mm mesiodistally and  
 118 3.6 mm labiolingually, dimensions similar to those observed in the dentary teeth of  
 119 *Psittacosaurus major* (You et al. 2008). The secondary ridges present on the labial  
 120 surface are less deeply incised than those on the lingual surface.

121

122 The apical margin of the crown exhibits a denticulate structure. The apical denticle,  
 123 along with two denticles located distal to the primary ridge and three denticles situated  
 124 mesial to the primary ridge, has been obliterated. The denticulated region extends  
 125 further basally along the distal carina than along the mesial carina (Fig. 2A, B). At least  
 126 nine denticles are observable on the mesial carina (Fig. 2), although the potential  
 127 absence of one denticle cannot be ruled out. On the distal carina, a minimum of 12  
 128 denticles are present (Fig. 2A, B and Fig. 3C, D), with the possibility that one denticle is  
 129 missing. In total, the dentary tooth has at least 22 denticles. The denticles located on the  
 130 distal carina near the base of the crown are displaced toward the lingual side, confluent  
 131 with the cingulum (Fig. 2A, B). The cingulum extends basomesially and is restricted to  
 132 the distal lobe (Fig. 2A, B).

133

134 As in some teeth of *Psittacosaurus xinjiangensis* (Sereno and Chao 1988), two  
135 distinct apical wear facets have been identified on the crown, oriented labially, and  
136 characterized by a flat morphology (Fig. 2C, D and Fig. 3C, D). The mesial apical facet  
137 is larger in size and positioned below the distal apical facet (Fig. 2C, D and Fig. 3C, D).  
138 The mesial apical facet forms an angle of approximately 35 degrees with respect to the  
139 vertical axis of the crown, whereas the distal apical facet creates an angle of  
140 approximately 50 degrees with the same vertical crown axis. Both of these angles are  
141 smaller than the 60 degrees observed in *P. xinjiangensis* (Sereno and Chao 1988).

142

143 Overlapping facets occur on both the mesial and distal surfaces (Fig. 3A, B, E, F).  
144 The distal overlapping facet is oriented distolingually, whereas the mesial overlapping  
145 facet is oriented labiomesially. The orientations of these two overlapping facets indicate  
146 imbricate arrangement between the crowns in this psittacosaur. The basal margins of the  
147 two overlapping facets are characterized by two linear segments that create an obtuse  
148 angle at their apical ends.

149

150 The labial surface of the crown exhibits a convex curvature in the mesiodistal  
151 direction and is nearly straight along the apicobasal direction (Fig. 3A–F). This  
152 morphology contrasts with the condition observed in *Psittacosaurus meileyingensis*  
153 (Sereno et al. 1988) and other ceratopsians (Chinnery et al. 1998), where the labial  
154 surface is convex in the apicobasal direction. Six labial secondary ridges are well  
155 preserved on the distal half, and extend basally to the midpoint of the crown (Fig. 2C, D  
156 and Fig. 3A, B). It is difficult to determine the presence of secondary ridges on the  
157 mesial half. There is a median depression toward the base on the labial crown surface  
158 (Fig. 2C, D).

159

160 The lingual surface of the crown is divided into a primary ridge, and the mesial and  
161 distal lobes (Fig. 2A, B). These lobes are approximately equal in size; however, the  
162 mesial lobe exhibits greater convexity compared to the distal lobe. As in other  
163 psittacosaurids (Sereno et al. 1988; Sereno 2010), a bulbous, median primary ridge  
164 occupies the center of the lingual surface (Fig. 2A, B). It angles slightly distally  
165 originates at the base of the crown, where it exhibits its greatest width, and narrows  
166 apically, to create a ridge (Fig. 2A, B). The primary ridge demonstrates a minor degree  
167 of asymmetry. The rounded crest of the ridge is located mesially, and the mesial edge of  
168 the ridge is more sharply delineated when contrasted with the distal edge, which is less  
169 clearly defined in relation to the rest of the crown (Fig. 2A, B). The primary ridge is  
170 covered by ten secondary ridges (Fig. 2A, B). Arranged from the mesial to the distal  
171 aspect, the first secondary ridge is the shortest, while the second is longer and wider  
172 than the first. The third secondary ridge is situated just apical to the second. The  
173 remaining ridges are of equal length, extending nearly the entire length of the primary  
174 ridge. Prominent and elongated grooves are present on the mesial and distal sides of the  
175 primary ridge. The mesial groove, originating at the base of the crown, angles distally,  
176 while the distal groove descends vertically, and is confluent with a resorbed groove

177 located on the root. Six secondary ridges extend a short distance down on the mesial  
178 lobe, with the ridge closest to the primary ridge basally against the primary ridge (Fig.  
179 2A, B). Four secondary ridges extend from the denticles on the distal lobe. The  
180 secondary ridge closest to the apical denticle basally terminates at the primary ridge,  
181 while the remaining ridges continue downward to the base of the crown (Fig. 2A, B).  
182 These ridges exhibit a rounded morphology.

183

184 **Root.** The root displays a subcylindrical morphology, characterized by a D-shaped  
185 cross-section, with the lingual aspect exhibiting a nearly linear configuration (Fig. 3G,  
186 H and Fig. 4C). The mesiodistal dimension of the root is approximately equal to its  
187 labiolingual width. The root surface is covered by a thin layer of cementum (Fig. 3G  
188 and Fig. 4), measuring approximately 40  $\mu\text{m}$  in thickness. The presence of cementum in  
189 PMOL-ADt0008 is consistent with occurrences reported in certain other ornithischian  
190 taxa (Erickson et al. 2012, 2015; LeBlanc et al. 2016; Bramble et al. 2017; Chen et al.  
191 2018). The mesial and distal surfaces of the root lack longitudinal grooves (Fig. 3A, B,  
192 E, F), a feature commonly observed in early-diverging neoceratopsians (He et al. 2018).  
193 Notably, two resorbed grooves are present in the central region of the lingual side of the  
194 root (Fig. 2A, B), indicating the presence of a resorption pit.

195

196 **Enamel.** Both the labial and lingual sides of the crown are coated with enamel;  
197 however, the enamel layer on the lingual side is notably thicker than that on the labial  
198 side (Fig. 4A), a pattern consistent with observations reported in the majority of  
199 psittacosaur species (Xu 1997; Tanoue et al. 2009; Sereno 2010). In contrast, the  
200 dentary teeth of *P. major* (You et al. 2008) and *P. gobiensis* (Sereno et al. 2010) display  
201 enamel on the lingual side but lack it on the labial side. Meanwhile, in *Psittacosaurus*  
202 sp., enamel thickness appears approximately equivalent on both the labial and lingual  
203 surfaces of the dentary teeth (Xu and Wang 1998).

204

205 **Dentine.** The dentine thickness is relatively uniform around the circumference at the  
206 base of the root. The dentine consists of an outer layer of high-density dentine and an  
207 inner layer of low-density dentine, with the junction between them clearly distinguished  
208 in CT rendered image (Fig. 4). This junction converges apically along the labiolingual  
209 direction (Fig. 4A), diverges externally along the mesiodistal direction (Fig. 4B), and  
210 exhibits a D-shaped cross-section (Fig. 4C). The thickness and volume of the  
211 high-density dentine are slightly greater than those of the low density dentine (Fig. 4C).  
212 At the base of the preserved root, the thickness of the high-density dentine is 0.44 mm,  
213 whereas that of the low-density dentine is 0.35 mm. Within the root, the low-density  
214 dentine contains a high density of small canals (Fig. 4C). In contrast, at the present  
215 resolution of 2.56  $\mu\text{m}$ , the crown dentine around the pulp chamber does not display  
216 discernible canals. However, it exhibits a low-attenuation signature consistent with the  
217 mineral density observed in the root's low-density dentine.

218

219 **Pulp cavity.** The pulp cavity is well-defined and distinctly divided into two  
220 components: the pulp chamber and the pulp canal (Fig. 5). The pulp chamber

221 constitutes the upper segment of the pulp cavity and is located within the crown of the  
222 tooth, while the pulp canal constitutes the lower segment of the pulp cavity, situated  
223 within the root. The pulp chamber has a chisel-like shape; it appears rectangular in the  
224 labial or lingual view and triangular in the mesial or distal view. Apically, mesioapically,  
225 and distoapically, several elongated canals diverge from the pulp chamber (Fig. 5),  
226 appearing along the mesiodistal plane of the crown. Similar canals are also present in a  
227 stegosaurian tooth (Skutschas et al. 2021). The dorsal margin of the pulp chamber is  
228 oriented mesioapically. The pulp canal is columnar, with a straight lingual side. Notably,  
229 densely small canals within the pulp cavity is restricted exclusively to the external  
230 surface of the pulp canal (Fig. 4A, B, C and Fig. 5). These canals are nearly parallel,  
231 radiating outward from the pulp cavity, and are not oriented strictly vertically relative to  
232 the pulp canal; instead, they are positioned at a slight apically oblique angle toward the  
233 apex (Fig. 5A–D). Their lengths vary (Fig. 5), with the maximum observed length  
234 reaching approximately 0.3 mm. For most of their length, the diameter of each canal is  
235 approximately 10  $\mu\text{m}$ . The basal diameters of these canals vary (Fig. 6), with maximum  
236 measurements of approximately 0.1 mm. The distances between different canals also  
237 vary (Fig. 6). Canal density was calculated per  $\text{mm}^2$ . The densities are approximately 43,  
238 47, 38, 40 canals per  $\text{mm}^2$  on the labial, lingual, mesial, and distal pulp cavity walls,  
239 respectively (Fig. 6). The average canal density in the pulp canal is 42 canals per  $\text{mm}^2$ .

240

## 241 Discussion

242

### 243 *Taxonomy and paleobiogeographic implications of PMOL-ADt0008*

244

245 PMOL-ADt0008, a left dentary tooth, can be attributed to the genus *Psittacosaurus*  
246 based on a diagnostic characteristic, the presence of a bulbous primary ridge (Sereno  
247 2010). To date, eleven valid species within this genus have been recognized. Among  
248 them, the number of marginal denticles on dentary teeth has traditionally been  
249 considered taxonomically informative. PMOL-ADt0008 exhibits at least 22 denticles,  
250 a condition most comparable to that of *P. xinjiangensis*, which displays relatively high  
251 denticle counts, reaching up to 21 (Sereno and Chao 1988). However, this apparent  
252 similarity should be interpreted with caution. Denticle number in *Psittacosaurus* is  
253 known to vary both ontogenetically and along the tooth row. For example, in *P.*  
254 *mongoliensis*, denticle counts increase during ontogeny (Sereno 1990), whereas in *P.*  
255 *xinjiangensis*, counts range from 13 to 21 depending on tooth position and individual  
256 variation (Brinkman et al. 2001). This variability diminishes the taxonomic reliability  
257 of denticle number as a sole diagnostic character. In addition to denticle number,  
258 PMOL-ADt0008 differs from *P. xinjiangensis* in several morphological aspects,  
259 including a distally inclined primary ridge and the lingual displacement of the  
260 distalmost denticles, which become confluent with the cingulum near the crown base.  
261 By contrast, in *P. xinjiangensis*, the primary ridge is typically vertical, and the distal  
262 denticles remain aligned along the carina (Sereno 1987; Brinkman et al. 2001).  
263 Nevertheless, the extent to which these differences exceed the range of intraspecific,  
264 positional, or ontogenetic variation remains unclear due to limited comparative data.

265 Stratigraphically, PMOL-ADt0008 was recovered from the same horizon as *P.*  
266 *meileyingensis*, suggesting a potential taxonomic affinity. However, *P. meileyingensis*  
267 is characterized by markedly lower denticle, with a count of 11 (Serenio et al. 1988),  
268 and it is uncertain whether this discrepancy can be fully explained by developmental  
269 or positional variation. Therefore, stratigraphic co-occurrence alone is insufficient to  
270 support a specific taxonomic assignment. Given the combined uncertainties related to  
271 character variability, limited comparative material, and the isolated nature of the  
272 specimen, a conservative taxonomic approach is warranted. Accordingly,  
273 PMOL-ADt0008 is best regarded as *Psittacosaurus* sp. pending the discovery and  
274 description of more complete material, particularly associated cranial or postcranial  
275 remains from the Longcheng locality, which may enable a more comprehensive  
276 systematic assessment.

277

278 The finding of PMOL-ADt0008 extends the known geographical distribution of  
279 psittacosaur in Jehol Biota. Psittacosaur are found only in the Lower Cretaceous of  
280 eastern Asia (Lucas 2006) and are common in the Jehol Biota (Zhao et al. 2007). In  
281 Jehol Biota, their fossils have been reported from the Yixian Formation at Sihetun and  
282 Lujiatun, Beipiao City, Liaoning Province (Ji and Bo 1998; Xu and Wang 1998; Zhou  
283 et al. 2006; Zhao et al. 2019), Bisiyingzi, Ningcheng County, Inner Mongolia (Zhang  
284 et al. 2022), and the Jiufotang Formation at Huanghuagou (Shijianggou), Chaoyang  
285 County, Liaoning Province (Serenio et al. 1988). The fossil studied here, found in the  
286 Jiufotang Formation at Shangshuaiquan Village, Longcheng District, Liaoning  
287 Province, indicates a new fossil site of psittacosaur within the Jehol Biota. It is  
288 important to note that the dinosaur assemblages at the Huanghuagou and  
289 Shangshuaiquan sites exhibit significant differences. The Shangshuaiquan site is  
290 characterized by the presence of large theropods, titanosauriforms (Yin et al. 2025),  
291 and *Psittacosaurus*, whereas the Huanghuagou site is limited to the occurrence of  
292 *Psittacosaurus* alone (Serenio et al. 1988). This disparity may reflect underlying  
293 paleoenvironmental conditions or potential sampling biases.

294

#### 295 *Dental variations of psittacosaur*

296

297 *Psittacosaurus* is the most species-rich genus among non-avian dinosaurs (Serenio  
298 2010), with hundreds to thousands of specimens reported from the Barremian to  
299 Albian of Asia (Serenio 2010; Serenio et al. 2010; Napoli et al. 2019; Podlesnov et al.  
300 2023). So far, at least 11 (and possibly as many as 19) species were named (Napoli et  
301 al. 2019; Ishikawa et al. 2025), while their systematic relationships and the validity of  
302 some species need to be further elaborated (Napoli et al. 2019). Notably, diagnostic  
303 features of *Psittacosaurus* species are mainly focused on the cranial skeleton, and the  
304 postcranial skeleton is generally very similar in *Psittacosaurus* (Serenio 1997). Yet,  
305 teeth have been received comparatively little attention on taxonomy in psittacosaur  
306 possibly due to the lack of thorough description for many species, but been shown to  
307 possess taxonomic value. For instance, the dentary teeth of *Psittacosaurus* exhibit a  
308 prominent bulbous primary ridge (Serenio 2010), whereas those of *P. xinjiangensis*

309 possess up to 21 denticles (Brinkman et al. 2001). Additionally, the maxillary teeth of  
310 *P. xinjiangensis* have crowns with denticulate margins that curve distolingually along  
311 the side near the crown base (Sereno and Chao 1988). In this context, the use of CT  
312 scanning on PMOL-ADt0008 provides more information in understanding variations  
313 of the dentary tooth of *Psittacosaurus* related to the primary ridge, median labial  
314 depression, the cingulum, and the distalmost denticles, which may facilitate the  
315 taxonomy and phylogenetic relationships of psittacosaur.

316

317 A prominent bulbous primary ridge on the dentary tooth crown constitutes a  
318 diagnostic feature of the genus *Psittacosaurus* (Sereno 2010). Nevertheless, the  
319 ornamentation and orientation of this ridge exhibit variation among different  
320 *Psittacosaurus* species. In PMOL-ADt0008, and *P. major* (You et al. 2008, fig. 5B),  
321 the bulbous primary ridge is ornamented with secondary ridges, whereas it appears  
322 smooth in *P. mongoliensis* (Sereno et al. 1988, fig. 7D). Regarding orientation, the  
323 bulbous primary ridge is vertically straight in *P. xinjiangensis* (Sereno 1987;  
324 Brinkman et al. 2001, fig. 3B), *P. meileyingensis* (Sereno et al. 1988, fig. 9A), and *P.*  
325 *mazongshanensis* (Xu 1997, fig. 4B), but it distally angles in PMOL-ADt0008, *P.*  
326 *mongoliensis* (Sereno et al. 1988, fig. 7D), and *P. houi* (Tanoue et al. 2009).  
327 Furthermore, the bulbous primary ridge exhibits asymmetry, with its rounded crest  
328 positioned more mesially in PMOL-ADt0008, *P. mongoliensis* (Sereno 1987) and *P.*  
329 *houi* (Tanoue et al. 2009, fig. 6D). Unfortunately, although the presence of the  
330 primary ridge has been reported in all species within the genus, the symmetry or  
331 asymmetry of this ridge remains undetermined in other *Psittacosaurus* species.

332

333 Other dental ornaments also exhibit significant variation. A median labial  
334 depression is present in PMOL-ADt0008, *P. xinjiangensis* (Sereno and Chao 1988;  
335 Brinkman et al. 2001), and *P. mongoliensis* (Sereno et al. 1988), but is absent in *P.*  
336 *gobiensis* (Sereno et al. 2010, fig. 3c) and *P. meileyingensis* (Sereno 1987). Notably,  
337 in PMOL-ADt0008 and *P. xinjiangensis* (Sereno 1987), this depression extends to the  
338 crown base, whereas it only reaches the midpoint in *P. mongoliensis* (Sereno 1987;  
339 Sereno et al. 1988, fig. 7D). Regarding the cingulum, PMOL-ADt0008 displays a  
340 derived state where the cingulum is restricted exclusively to the distal lobe, differing  
341 from the bilateral distribution (mesial and distal) observed in *P. houi* and other  
342 early-diverging ceratopsians like *Yinlong* and *Leptoceratops* (Tanoue et al. 2009).  
343 Most distinctively, the distal denticles near the crown base in PMOL-ADt0008 are  
344 lingually displaced and confluent with the cingulum. This morphological  
345 configuration has not been reported in other psittacosaur specimens, representing a  
346 potentially diagnostic feature of this taxon.

347

348 Despite the considerable taxonomic and phylogenetic potential of these dental  
349 characteristics, a cautious approach is warranted. To date, no studies have sufficiently  
350 examined the influence of individual variation, positional differences, or ontogenetic  
351 changes on these features in psittacosaur. Until these factors are more thoroughly  
352 understood, the incorporation of these dental traits into taxonomic frameworks should be

353 undertaken with care.

354

355 *Pulp cavity in ceratopsians*

356

357 To date, the three-dimensional internal morphology of the ceratopsian pulp cavity has  
358 remained entirely uncharacterized. By utilizing ultra-high-resolution micro-CT data, this  
359 study successfully visualizes these internal structures for the first time, defining  
360 morphological details down to the 10  $\mu\text{m}$  scale of individual canals. The pulp chamber  
361 exhibits a chisel-shaped morphology, whereas the pulp canal is columnar in form. Within  
362 the apical region of the pulp chamber, multiple elongated canals are present. Additionally,  
363 the pulp canal contains densely small canals that penetrate the dentine to varying degrees.  
364 These canals have a diameter of approximately 10  $\mu\text{m}$  and are nearly parallel to one  
365 another. Further dental histological sectioning is necessary to definitively identify their  
366 nature. Finally, the functional implications of the pulp cavity structure remain speculative.  
367 Future research utilizing biomechanical methods, such as finite element analysis (FEA), is  
368 required to quantitatively validate how this structure responded to vertical and horizontal  
369 jaw movements.

370

## 371 **Conclusions**

372

373 This study documents the discovery of a dentary tooth of *Psittacosaurus* from the  
374 Lower Cretaceous Jiufotang Formation, representing a new fossil locality for  
375 psittacosaurus within the Jehol Biota at Longcheng, western Liaoning. The specimen  
376 is provisionally assigned to *Psittacosaurus* sp. based on the presence of a bulbous  
377 primary ridge and a distinctive combination of crown features, while acknowledging  
378 the taxonomic limitations inherent to its isolated nature and potential intraspecific  
379 variation. High-resolution micro-computed tomography provides the first  
380 three-dimensional reconstruction of ceratopsian dental internal anatomy, revealing a  
381 bipartite pulp cavity composed of a chisel-shaped pulp chamber and a columnar pulp  
382 canal. These findings expand current understanding of dental morphological variation  
383 in *Psittacosaurus*, underscore the limited taxonomic reliability of isolated dental  
384 characters, and demonstrate the potential of non-destructive imaging techniques to  
385 reveal previously inaccessible anatomical information relevant to ceratopsian  
386 evolution.

387

## 388 **Acknowledgements**

389

390 We thank Qiang Yang (Paleontological Museum of Liaoning, Shenyang) for his  
391 help in collecting and preparing the tooth.

392

## 393 **References**

394

395 Bramble K, LeBlanc ARH, Lamoureux DO, Wosik M, Currie PJ (2017) Histological  
396 evidence for a dynamic dental battery in hadrosaurid dinosaurs. Scientific

- 397 Reports 7(1): 15787. <https://doi.org/10.1038/s41598-017-16056-3>  
398
- 399 Brinkman DB, Eberth DA, Ryan MJ, Chen PJ (2001) The occurrence of  
400 *Psittacosaurus xinjiangensis* Sereno and Chow, 1988 in the Urho area, Junggar  
401 Basin, Xinjiang, People's Republic of China. Canadian Journal of Earth Sciences  
402 38(12): 1781–1786. <https://doi.org/10.1139/e01-049>  
403
- 404 Bullar CM, Zhao Q, Benton MJ, Ryan MJ (2019) Ontogenetic braincase development  
405 in *Psittacosaurus lujiatunensis* (Dinosauria: Ceratopsia) using micro-computed  
406 tomography. PeerJ 7: e7217. <https://doi.org/10.7717/peerj.7217>  
407
- 408 Chen J, LeBlanc ARH, Jin LY, Huang T, Reisz RR (2018) Tooth development,  
409 histology, and enamel microstructure in *Changchunsaurus parvus*: Implications  
410 for dental evolution in ornithomimid dinosaurs. PLoS ONE 13(11):  
411 e0205206. <https://doi.org/10.1371/journal.pone.0205206>  
412
- 413 Chinnery BJ, Lipka TR, Kirkland JI, Parrish JM, Brett-Surman MK (1998)  
414 Neoceratopsian teeth from the Lower to Middle Cretaceous of North America. In:  
415 Lucas SG, Kirkland JI, Estep JW (Eds) Lower and Middle Cretaceous Terrestrial  
416 Ecosystems. New Mexico Museum of Natural History and Science Bulletin No.  
417 14, New Mexico, 297–302.  
418
- 419 Erickson GM, Krick BA, Hamilton M, Bourne GR, Norell MA, Lilleodden E, Sawyer  
420 WG (2012) Complex dental structure and wear biomechanics in hadrosaurid  
421 dinosaurs. Science 338(6103): 98–101. <https://doi.org/10.1126/science.1224495>  
422
- 423 Erickson GM, Sidebottom MA, Kay DI, Turner KT, Ip N, Norell MA, Sawyer WG,  
424 Krick BA (2015) Wear biomechanics in the slicing dentition of the giant horned  
425 dinosaur *Triceratops*. Science Advances 1(5): e1500055.  
426 <https://doi.org/10.1126/sciadv.1500055>  
427
- 428 He YM, Makovicky PJ, Xu X, You HL (2018) High-resolution computed tomographic  
429 analysis of tooth replacement pattern of the basal neoceratopsian *Liaoceratops*  
430 *yanzigouensis* informs ceratopsian dental evolution. Scientific Reports 8: 5870.  
431 <https://doi.org/10.1038/s41598-018-24283-5>  
432
- 433 Ishikawa A, Zheng WJ, Imai T, Hattori S, Shibata M, Kawabe S, Jin XS (2025)  
434 *Psittacosaurus houi*, a longer snouted psittacosaurid from the Lower Cretaceous  
435 Lujiatun Unit of Yixian Formation, China, with the synonymy of the unresolved  
436 genus *Hongshanosaurus* revisited. PeerJ 13: e19547.  
437 <https://doi.org/10.7717/peerj.19547>  
438
- 439 Ji SA, Bo HC (1998) Discovery of the psittacosaurid skin impressions and its  
440 significance. Geological Review 44(6): 603–606 (in Chinese with English

441 abstract).

442

443 LeBlanc ARH, Reisz RR, Evans DC, Bailleul AM (2016) Ontogeny reveals function  
444 and evolution of the hadrosaurid dinosaur dental battery. *BMC Evolutionary*  
445 *Biology* 16(1): 152. <https://doi.org/10.1186/s12862-016-0721-1>

446

447 Lucas SG (2006) The *Psittacosaurus* biochron, Early Cretaceous of Asia. *Cretaceous*  
448 *Research* 27: 189–198. <https://doi.org/10.1016/j.cretres.2005.11.011>

449

450 Marsh OC (1890) Description of new dinosaurian reptiles. *American Journal of*  
451 *Science (Third Series)* 39: 81–86.

452

453 Mayr G, Peters DS, Plodowski G, Vogel O (2002) Bristle-like integumentary  
454 structures at the tail of the horned dinosaur *Psittacosaurus*. *Naturwissenschaften*  
455 89(8): 361–365. <https://doi.org/10.1007/s00114-002-0339-6>

456

457 Napoli JG, Hunt T, Erickson GM, Norell MA (2019) *Psittacosaurus amitabha*, a new  
458 species of ceratopsian dinosaur from the Ondai Sayr locality, central Mongolia.  
459 *American Museum Novitates* 3932: 1–36. <https://doi.org/10.1206/3932.1>

460

461 Osborn HF (1923) A new genus and species of Ceratopsia from New Mexico,  
462 *Pentaceratops sternbergii*. *American Museum Novitates* 93: 1–3.

463

464 Owen R (1842) Report on British fossil reptiles, Part II. Report of the British  
465 Association for the Advancement of Science 11: 60–204.

466

467 Podlesnov AV, Averianov AO, Burukhin AA, Feofanova OA, Vladimirova ON (2023)  
468 New data on skull morphology of *Psittacosaurus sibiricus* (Dinosauria:  
469 Ceratopsia) using micro-computed tomography. *Paleontological Journal* 57(10):  
470 1128–1187. <https://doi.org/10.1134/S0031030123100040>

471

472 Russell DA, Zhao XJ (1996) New psittacosaur occurrences in Inner Mongolia.  
473 *Canadian Journal of Earth Sciences* 33(4): 637–648.  
474 <https://doi.org/10.1139/e96-047>

475

476 Seeley HG (1887) On the classification of the fossil animals commonly named  
477 Dinosauria. *Proceedings of the Royal Society of London* 43: 165–171.

478

479 Sereno PC (1987) The ornithischian dinosaur *Psittacosaurus* from the Lower  
480 Cretaceous of Asia and the relationships of the Ceratopsia. PhD Thesis,  
481 Columbia University, New York, The United States of America.

482

483 Sereno PC (1990) New data on parrot-beaked dinosaurs (*Psittacosaurus*). In:  
484 Carpenter K, Currie PJ (Eds) *Dinosaur Systematics: Approaches and*

- 485 Perspectives. Cambridge University Press, Cambridge, 203–210.
- 486
- 487 Sereno PC (1997) Psittacosauridae. In: Currie PJ, Padian K (Eds) Encyclopedia of  
488 Dinosaurs. Academic Press, San Diego, 611–613.
- 489
- 490 Sereno PC (2010) Taxonomy, cranial morphology, and relationships of parrot-beaked  
491 dinosaurs (Ceratopsia: Psittacosaurus). In: Ryan MJ, Chinnery-Allgeier BJ,  
492 Eberth DA (Eds) New Perspectives on Horned Dinosaurs: The Royal Tyrrell  
493 Museum Ceratopsian Symposium, Drumheller, Alberta (Canada), September  
494 2007. Indiana University Press, Bloomington, 21–58.
- 495
- 496 Sereno PC, Chao SC (1988) *Psittacosaurus xinjiangensis* (Ornithischia: Ceratopsia), a  
497 new psittacosaur from the Lower Cretaceous of northwestern China. Journal of  
498 Vertebrate Paleontology 8(4): 353–365.  
499 <https://doi.org/10.1080/02724634.1988.10011724>
- 500
- 501 Sereno PC, Zhao XJ, Tan L (2010) A new psittacosaur from Inner Mongolia and the  
502 parrot-like structure and function of the psittacosaur skull. Proceedings of the  
503 Royal Society B: Biological Sciences 277(1679): 199–209.  
504 <https://doi.org/10.1098/rspb.2009.0691>
- 505
- 506 Sereno PC, Chao SC, Cheng ZW, Rao CG (1988) *Psittacosaurus meileyingensis*  
507 (Ornithischia: Ceratopsia), a new psittacosaur from the Lower Cretaceous of  
508 northeastern China. Journal of Vertebrate Paleontology 8(4): 366–377.  
509 <https://doi.org/10.1080/02724634.1988.10011725>
- 510
- 511 Skutschas PP, Kolchanov VV, Gardner JD (2021) Microanatomy and histology of  
512 frontal bones in two species of *Albanerpeton* sensu lato (Lissamphibia:  
513 Albanerpetontidae) from the Upper Cretaceous Oldman Formation in  
514 southeastern Alberta, Canada. Historical Biology 33(12): 3604–3616.  
515 <https://doi.org/10.1080/08912963.2021.1881084>
- 516
- 517 Tanoue K, Grandstaff BS, You HL, Dodson P (2009) Jaw mechanics in basal  
518 Ceratopsia (Ornithischia, Dinosauria). The Anatomical Record 292(9):  
519 1352–1369. <https://doi.org/10.1002/ar.20979>
- 520
- 521 Xu X (1997) A new psittacosaur (*Psittacosaurus mazongshanensis* sp. nov.) from  
522 Mazongshan area, Gansu Province, China. In: Dong ZM (Ed.) Sino-Japanese  
523 Silk Road Dinosaur Expedition. China Ocean Press, Beijing, 48–67.
- 524
- 525 Xu X, Wang XL (1998) New psittacosaur (Ornithischia, Ceratopsia) occurrence from  
526 the Yixian Formation of Liaoning, China and its stratigraphical significance.  
527 Vertebrata Palasiatica 36(2): 147–158 (in Chinese with English abstract).  
528 <https://www.vertpala.ac.cn/EN/Y1998/V36/I02/147>

529

530 Yin YL, Li Y, Hu J, Zhang HG (2025) Dinosaur teeth from the Lower Cretaceous  
531 Jiufotang Formation of western Liaoning, China. PeerJ 13: e19013.  
532 <https://doi.org/10.7717/peerj.19013>

533

534 You HL, Dodson P (2004) Basal Ceratopsia. In: Weishampel DB, Dodson P,  
535 Osmolska H (Eds) The Dinosauria (Second Edition). University of California  
536 Press, Berkeley, 478–493.  
537 <https://doi.org/10.1525/california/9780520242098.003.0025>

538

539 You HL, Tanoue K, Dodson P (2008) New data on cranial anatomy of the ceratopsian  
540 dinosaur *Psittacosaurus major*. Acta Palaeontologica Polonica 53(2): 183–196.  
541 <https://doi.org/10.4202/app.2008.0202>

542

543 Zhang HG, Yu DX, Feng YH, Pei R, Zhou CF (2022) A Lujiatun-like dinosaurian  
544 assemblage from the Jehol Biota of Ningcheng, Inner Mongolia, Northeast China.  
545 Acta Palaeontologica Polonica 67(3): 617–621.  
546 <https://doi.org/10.4202/app.00975.2022>

547

548 Zhao Q, Barrett PM, Eberth DA (2007) Social behaviour and mass mortality in the  
549 basal ceratopsian dinosaur *Psittacosaurus* (Early Cretaceous, People's Republic  
550 of China). Palaeontology 50(5): 1023–1029.  
551 <https://doi.org/10.1111/j.1475-4983.2007.00709.x>

552

553 Zhao Q, Benton MJ, Xu X, Sander PM (2014) Juvenile-only clusters and behaviour of  
554 the Early Cretaceous dinosaur *Psittacosaurus*. Acta Palaeontologica Polonica  
555 59(4): 827–833. <https://doi.org/10.4202/app.2012.0128>

556

557 Zhao Q, Benton MJ, Hayashi S, Xu X (2019) Ontogenetic stages of ceratopsian  
558 dinosaur *Psittacosaurus* in bone histology. Acta Palaeontologica Polonica 64(2):  
559 323–334. <https://doi.org/10.4202/app.00559.2018>

560

561 Zhao Q, Benton MJ, Sullivan C, Sullivan PM, Xu X (2013) Histology and postural  
562 change during the growth of the ceratopsian dinosaur *Psittacosaurus*  
563 *lujiatunensis*. Nature Communications 4(1): 2079.  
564 <https://doi.org/10.1038/ncomms3079>

565

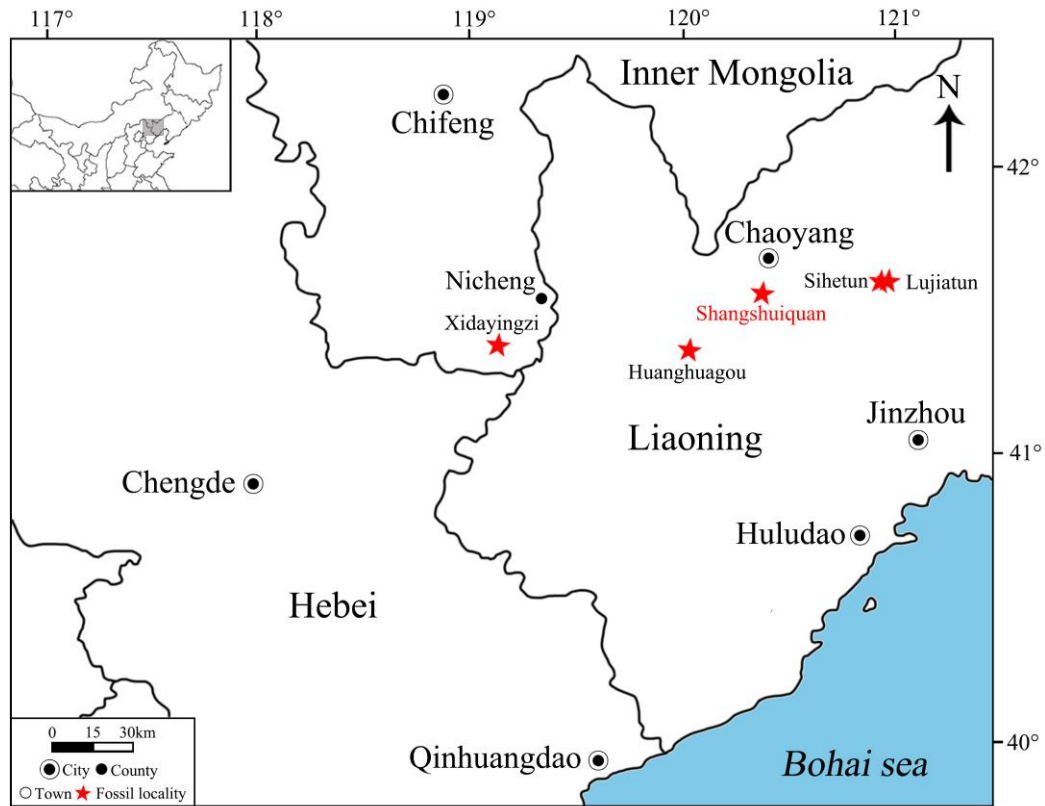
566 Zhou CF, Gao KQ, Fox RC, Chen SH (2006) A new species of *Psittacosaurus*  
567 (Dinosauria: Ceratopsia) from the Early Cretaceous Yixian Formation, Liaoning,  
568 China. Palaeoworld 15(1): 100–114.  
569 <https://doi.org/10.1016/j.palwor.2005.11.001>

570

571 **Figure captions**

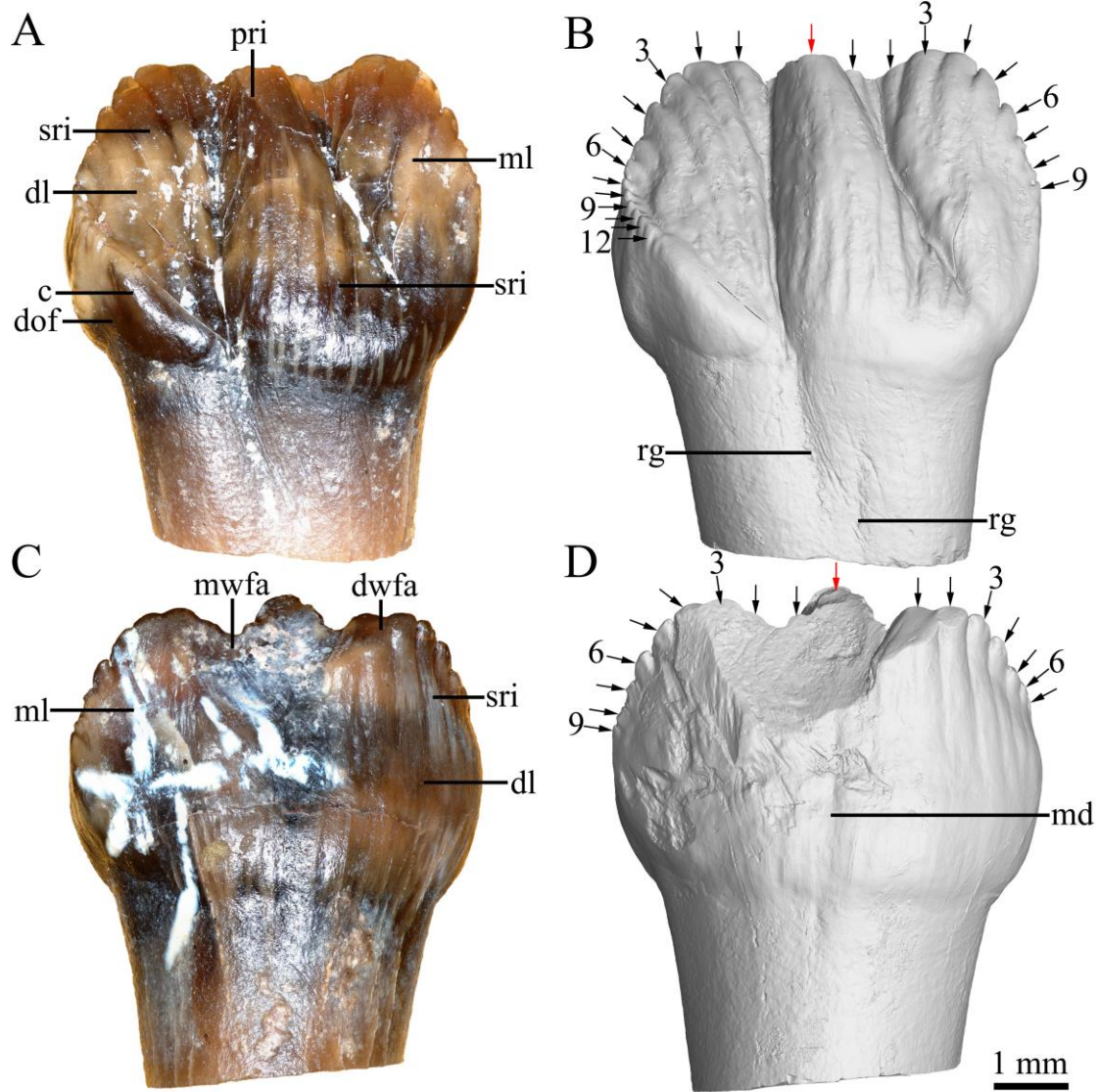
572

573 **Figure 1.** Map showing fossil site of *Psittacosaurus* sp. (PMOL-ADt0008) in  
574 Shangshuiquan, Lianhe, Longcheng, Chaoyang, western Liaoning, China.



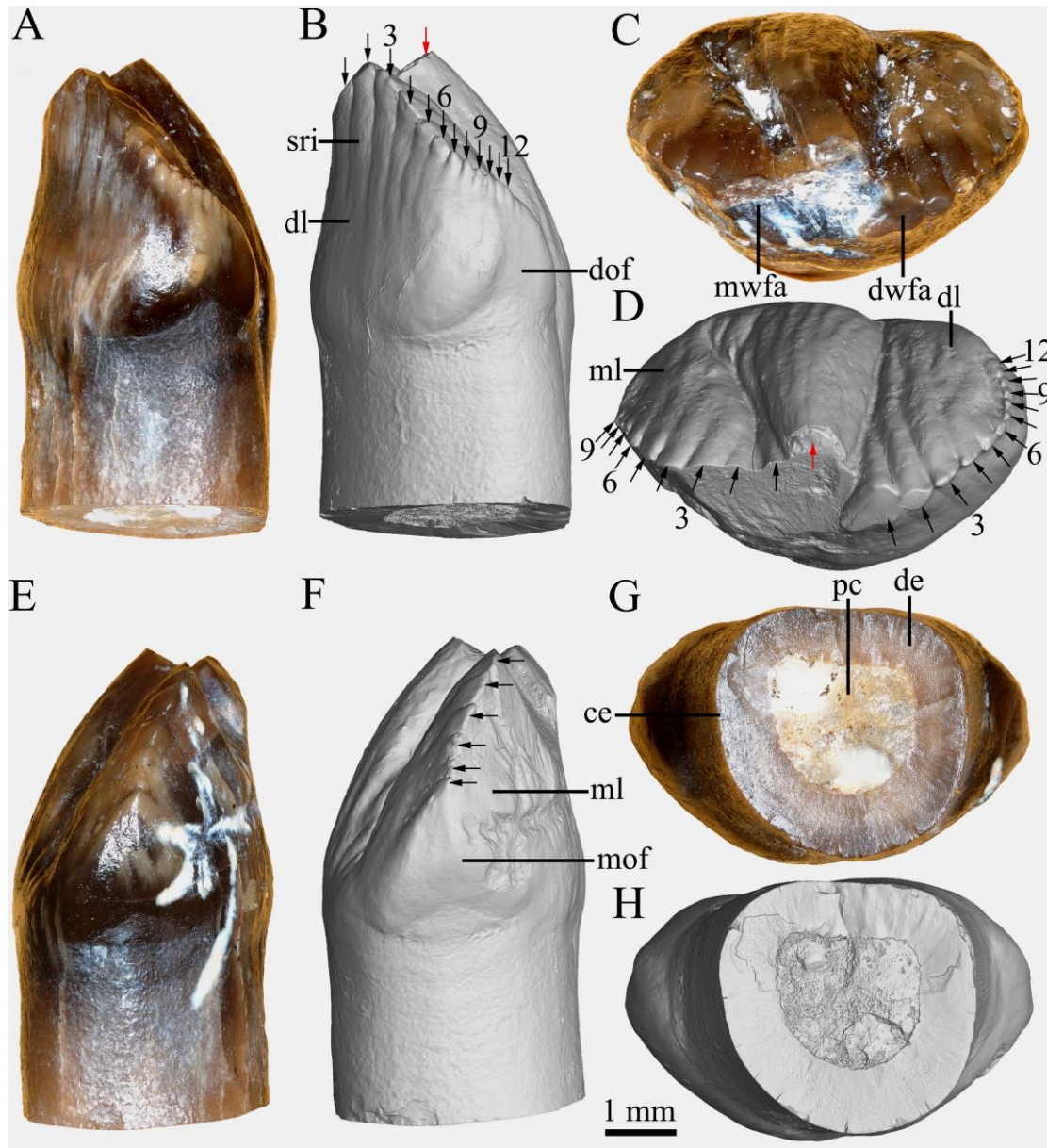
575

576 **Figure 2.** The left dentary tooth (PMOL-ADt0008) of a psittacosaur in lingual (**A, B**),  
577 labial (**C, D**) views. Abbreviations: c, cingulum; dl, distal lobe; dwfa, distal wear facet;  
578 dof, distal overlapping facet; md, median depression; ml, mesial lobe; mwfa, mesial wear facet;  
579 pri, primary ridge; rg, resorbed groove; sri, secondary ridge. The red arrow  
580 indicates the apical denticle, while the black arrows indicate the other denticles.

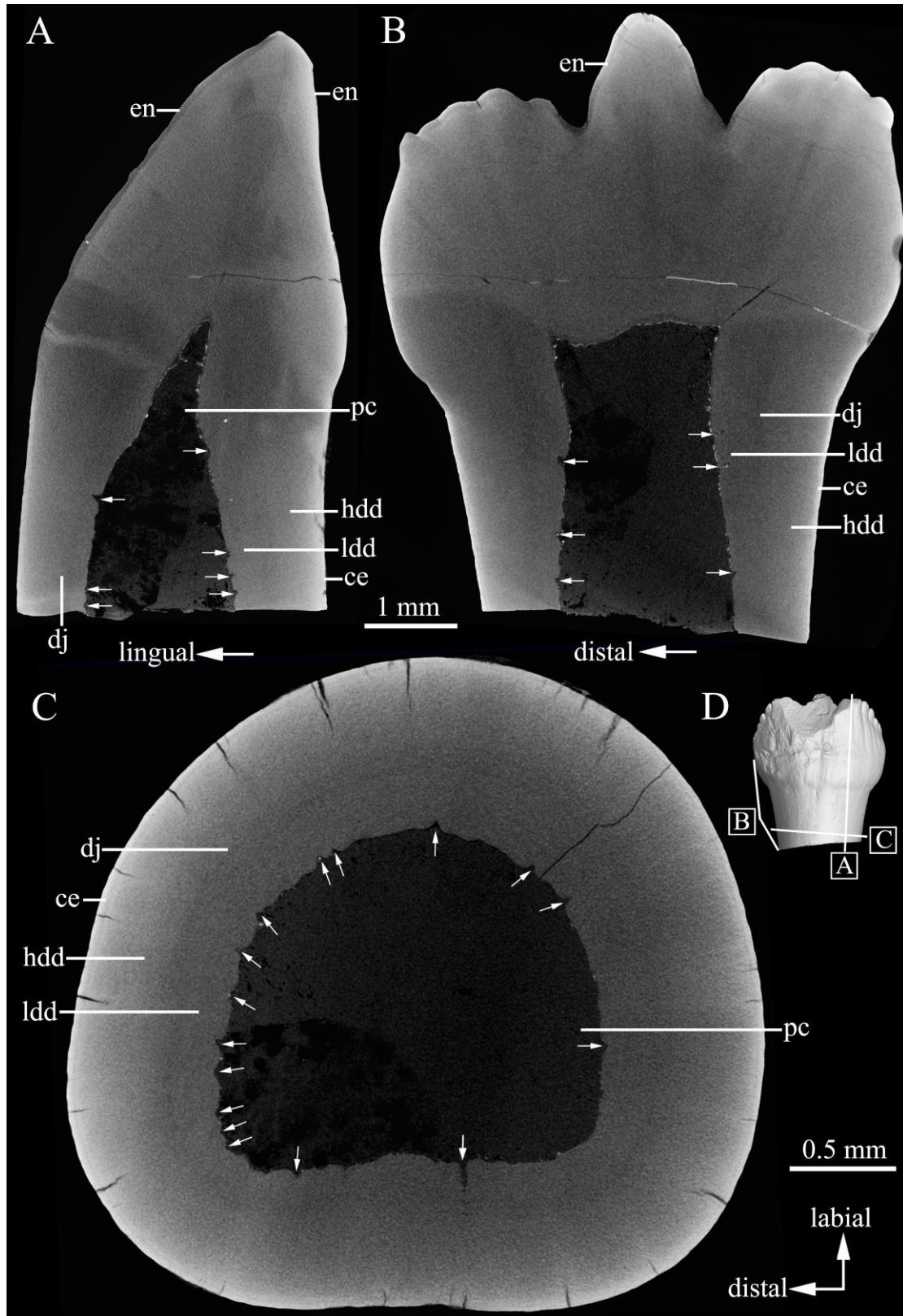


581

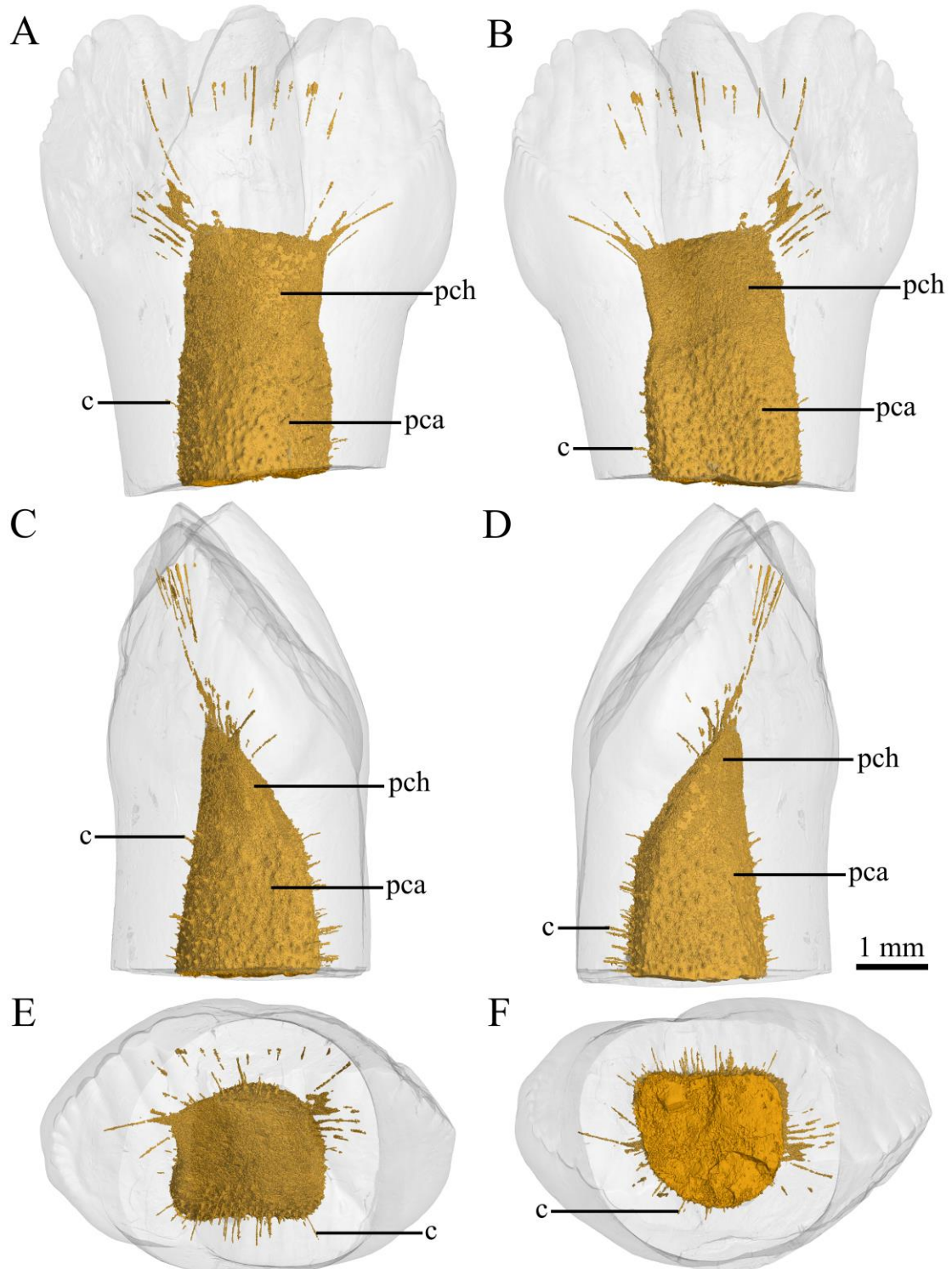
582 **Figure 3.** The left dentary tooth (PMOL-ADt0008) of a psittacosaur in distal (**A, B**),  
 583 apical (**C, D**), mesial (**E, F**), and basal (**G, H**) views. Abbreviations: ce, cementum; de,  
 584 dentine; dl, distal lobe; dwfa, distal wear facet; dof, distal overlapping facet; ml,  
 585 mesial lobe; mwfa, mesial wear facet; mof, mesial overlapping facet; pc, pulp cavity;  
 586 sri, secondary ridge. The red arrow indicates the apical denticle, while the black  
 587 arrows indicate the other denticles.



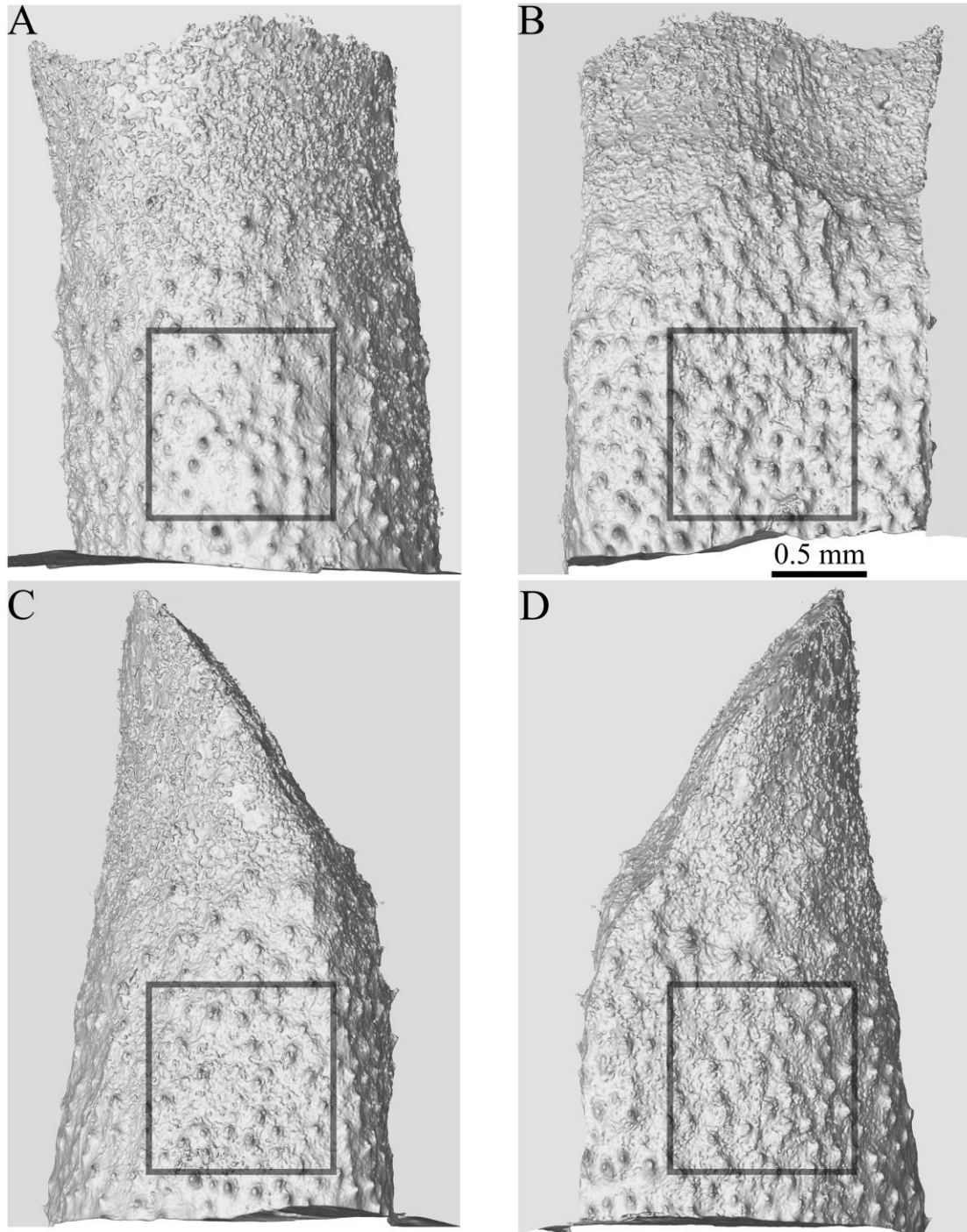
589 **Figure 4.** CT rendered images of the left dentary tooth (PMOL-ADt0008) of a  
 590 psittacosaur in labial view (C) with selected sections (A, B, D). Abbreviations: ce,  
 591 cementum; de, dentine; dj, density junction; en, enamel; hdd, high-density dentine;  
 592 ldd, low-density dentine; pc, pulp cavity. White arrows indicate canals.



594 **Figure 5.** CT rendered images of the left dentary tooth (PMOL-ADt0008) of a  
595 psittacosaur, highlighting the pulp cavity in lingual (**A**), labial (**B**), distal (**C**), mesial  
596 (**D**), apical (**E**), and basal (**F**) views. Abbreviations: c, canal; pca, pulp canal; pch,  
597 pulp chamber.



599 **Figure 6.** CT rendered images of the left dentary tooth (PMOL-ADt0008) of a  
600 psittacosaur, showing canals, in labial (A), lingual (B), mesial (C), and distal (D)  
601 walls of the pulp cavity. The area of the region where the square is located is 1 mm<sup>2</sup>.



602